Supporting Information for

High-Twist-Pervaded Electrochemical Yarn Muscles with Ultralarge and Fast Contractile Actuations

Yulian Wang, Jian Qiao, Kunjie Wu, Wei Yang, Ming Ren, Lizhong Dong, Yurong Zhou, Yulong Wu, Xiaona Wang, Zhenzhong Yong, Jiangtao Di, and Qingwen Li

Y. Wang, M. Ren, L. Dong, Y. Zhou, Prof. J. Di, Prof. Q. Li
School of Nano-Technology and Nano-Bionics, University of Science and Technology of China, Hefei 230026, China

Y. Wang, J. Qiao, Dr. K. Wu, Dr. W. Yang, M. Ren, L. Dong, Y. Zhou, Dr. Y. Wu, Dr. X. Wang, Prof. J. Di, Prof. Q. Li
Key Laboratory of Multifunctional Nanomaterials and Smart Systems, Advanced Materials Division, Suzhou Institute of Nano-Tech and Nano-Bionics, Chinese Academy of Sciences, Suzhou 215123, China
E-mail: jtdi2009@sinano.ac.cn, qwli2007@sinano.ac.cn

Dr. K. Wu, Dr. Z. Yong, Prof. Q. Li
Division of Nanomaterials, Suzhou Institute of Nano-Tech and Nano-Bionics, Chinese Academy of Sciences, Nanchang 330200, China

Keywords: Actuators, Artificial muscles, Carbon nanotube, Supercapacitor, Electrochemistry

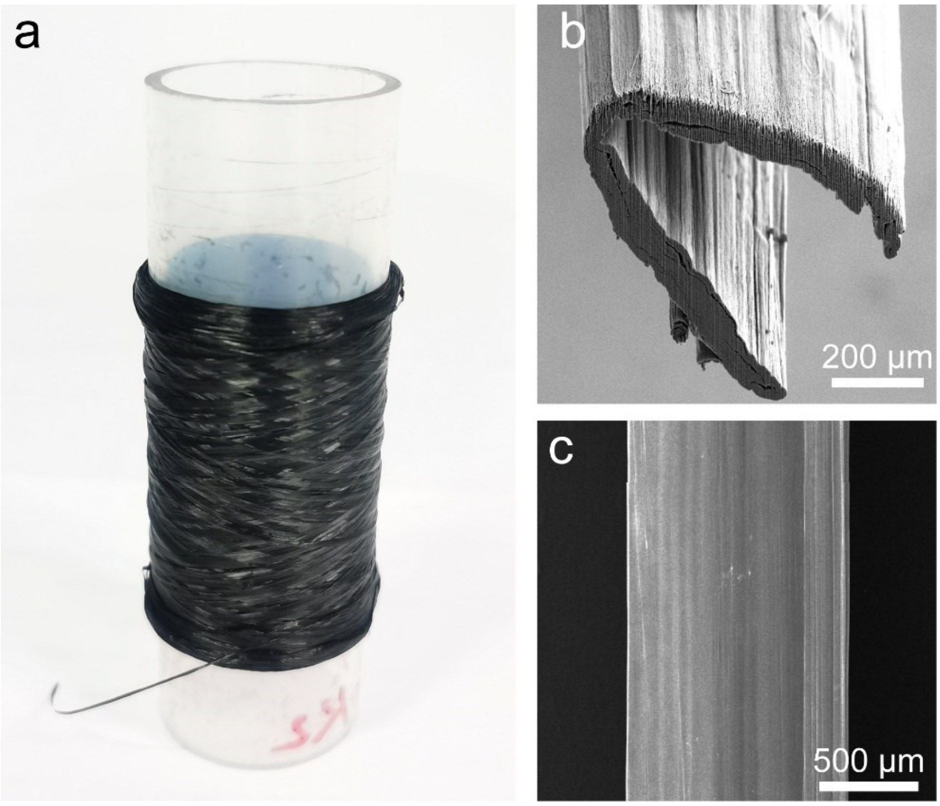

Figure S1. (a) Photograph a hundreds-meter-long CNT ribbon winded on a mandrel. (b) SEM images of the cross-section of a CNT ribbon, indicating a thin and narrow film. The ribbon was cut by a focused gallium ion beam perpendicular to the length direction of the ribbon. (c) SEM image of the surface of a CNT ribbon. The CNT ribbon results from the densification of an as-grown CNT aerogel sheet by water.

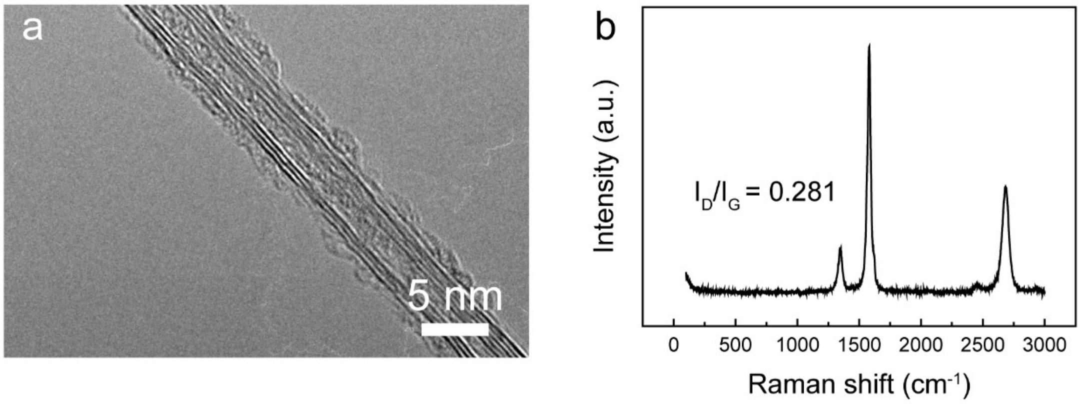

Figure S2. (a) TEM image of typical CNTs in the ribbon, showing the CNTs have 2-5 graphitic walls and a diameter of about 5 nm. (b) Raman spectrum of the CNT ribbon.

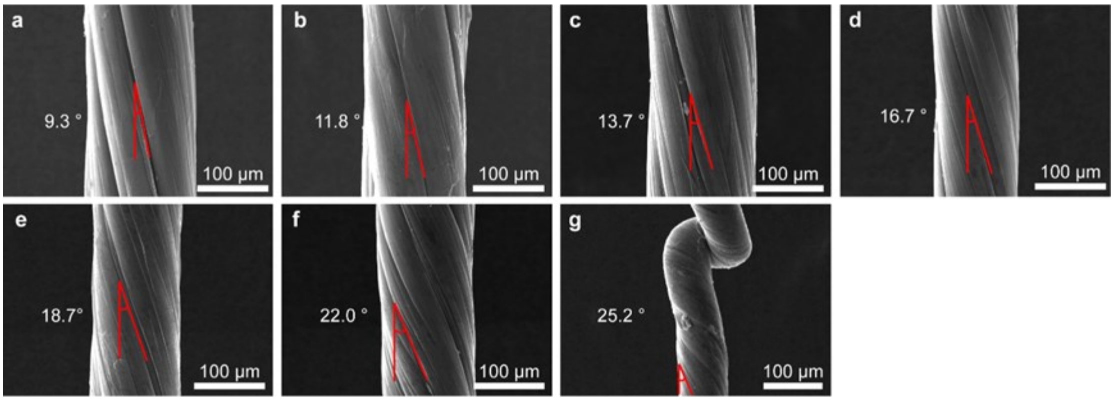

Figure S3. SEM images of the twisted component CNT yarns with different bias angles from 9.3° to 22.0°. The relationship between bias angle and twist density for these yarns was shown in Fig. S10a. The maximum bias angle we achieved was about 22° at which the yarn that was under a tension of 4 MPa could remain straight. Further increasing the bias angle by adding twists was failed due to the starting of coiling as shown in (g).

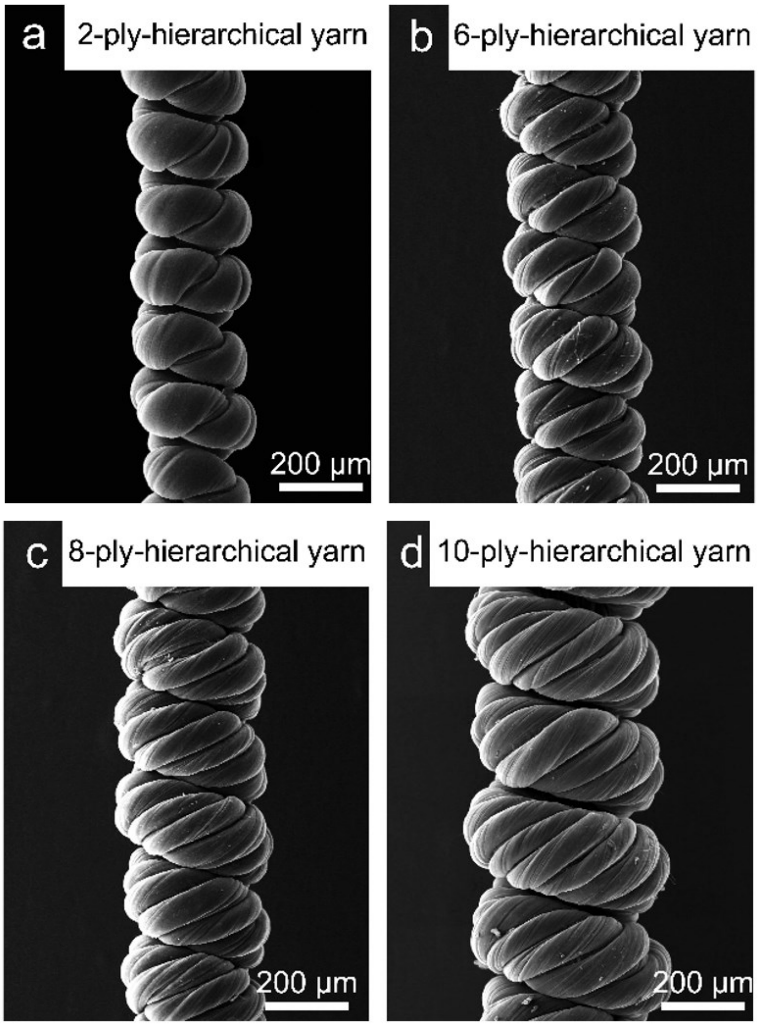

Figure S4. SEM images of (a) 2-ply, (b) 6-ply, (c) 8-ply, and (d) 10-ply hierarchical CNT yarns.

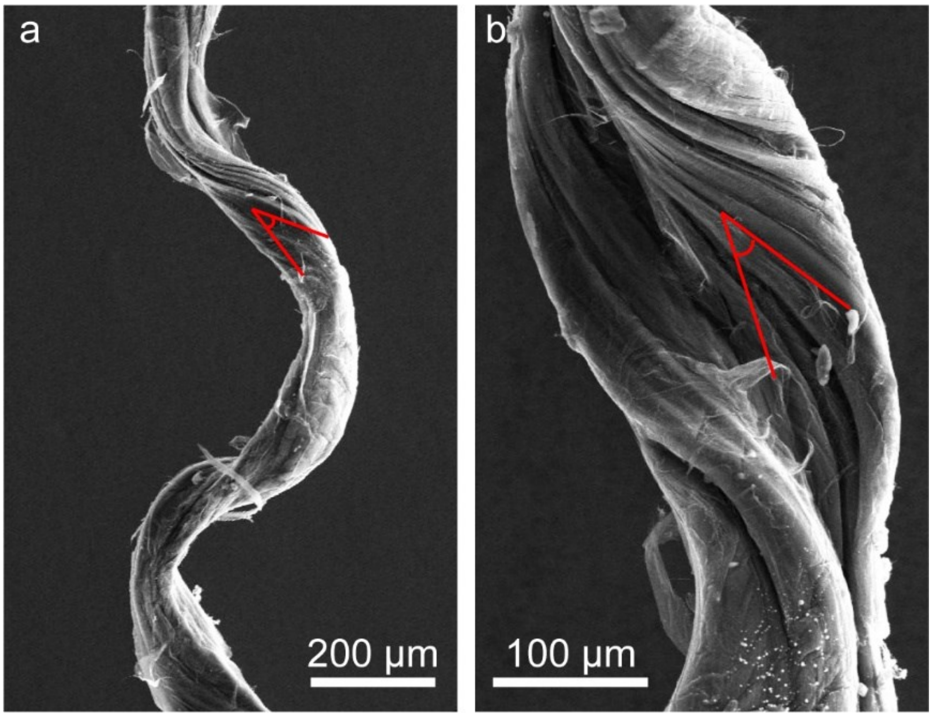

Figure S5. SEM images of an individual component CNT yarn that was separated from a 4-ply coiled hierarchical yarn by hand disassembling at (a) low and (b) high magnifications. The red lines indicate the presence of the twisted structure at the side close to the center of the 4-ply yarn. The component yarn was densified by the twisting that was applied during spinning the 4-ply yarn.

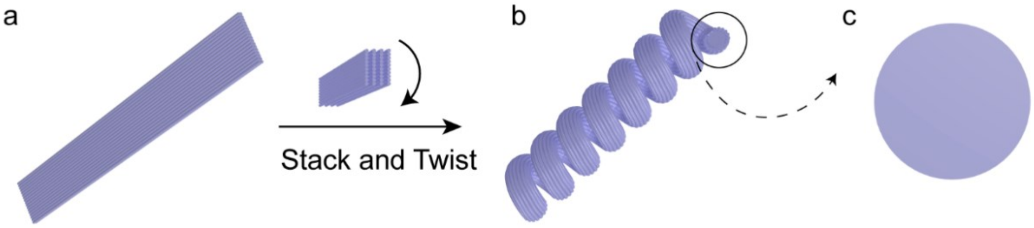

Figure S6. Schematic showing the steps for the fabrication of 4-ply merged yarn muscles. Four CNT ribbons are stacked together, followed by counterclockwise twisting to form a coiled yarn.

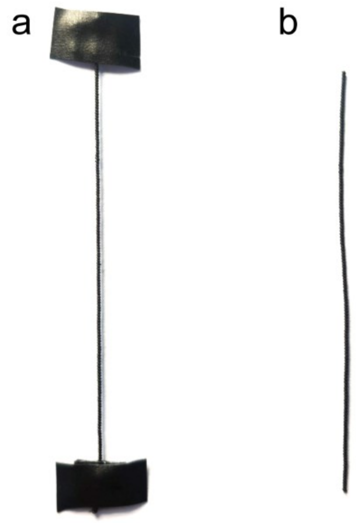

Figure S7. Photographs of (a) a two-end-tethered 4-ply hierarchical yarn and (b) the yarn after moving the tethering, indicating that the 4-ply hierarchical yarn is twist-stable.

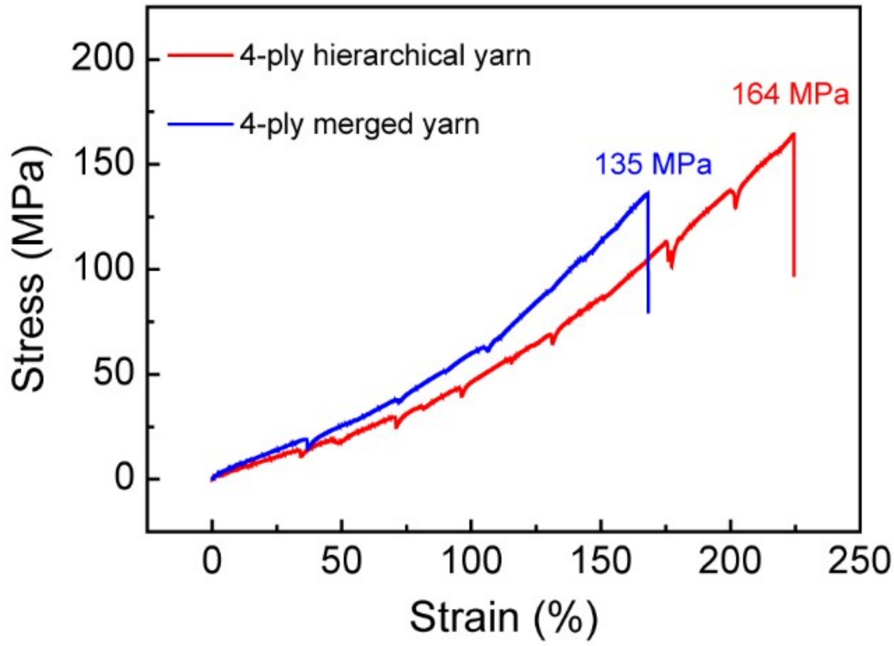

Figure S8. The Stress-strain curves of the 4-ply hierarchical and the 4-ply merged yarns.

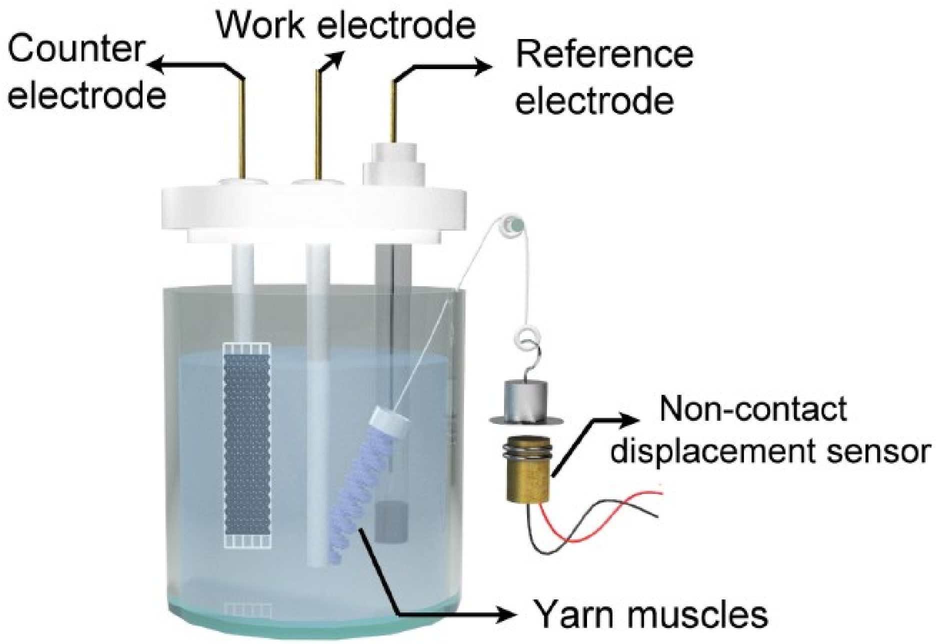

Figure S9. Schematic showing the apparatus utilized for actuation characterization. The test is conducted in 0.2 M TEA·BF_4 dissolved in PC using a three-electrode configuration, where a coiled CNT yarn muscle works as the working electrode, an Ag/Ag^{+} as the reference electrode, and a Pt mesh with CNT film as the counter electrode. Muscle contraction is measured by a contactless displacement sensor.

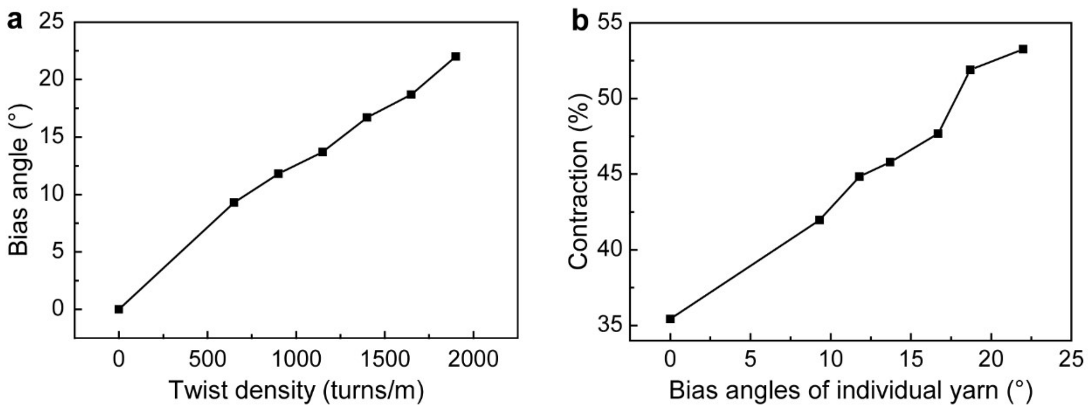

Figure S10. (a) The bias angle as a function of twist density for the twisted yarn shown in Fig. S3. (b) The dependence of the contraction generated by the 4-ply-hierarchial yarn muscles on the bias angle observed on the twisted component yarns used for preparing the corresponding hierarchical yarn muscles.

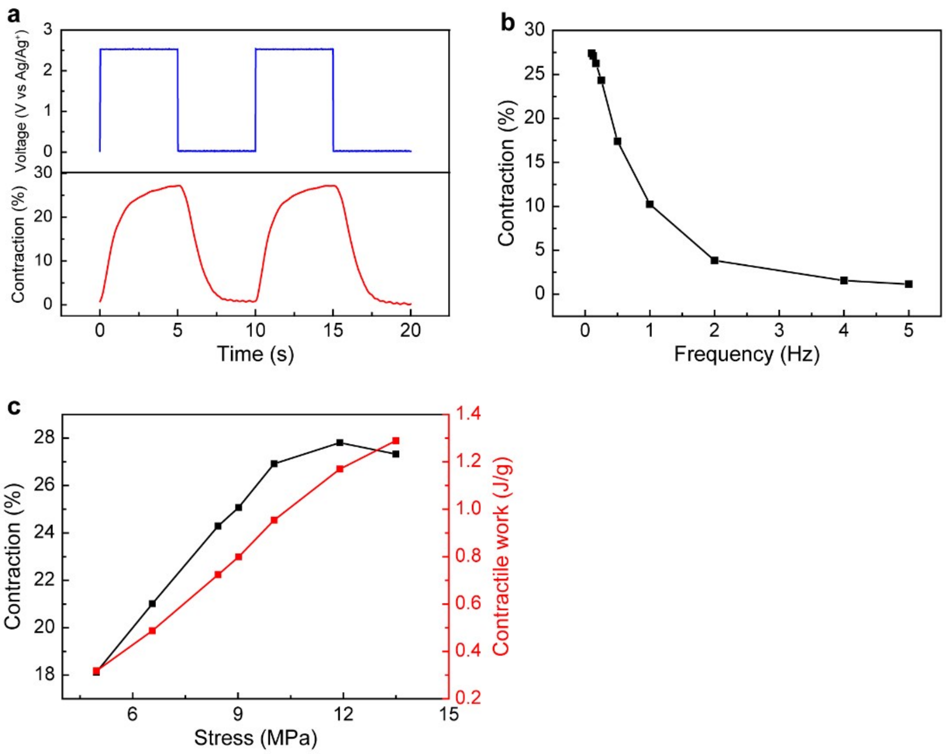

Figure S11. Characterization of electrochemical actuation of single coiled CNT yarn muscles. (a) Contraction response upon square-wave voltage signals. (b) The dependence of tensile contractions on voltage on-off frequency for single yarn muscles. The voltage is 2.5 V and the applied stress is 10 MPa. (c) The stress dependence of muscle contraction (left axis) and contractile work (right axis) of the single coiled CNT yarn muscles, while the applied square-wave potential was 2.5 V vs Ag/Ag^{+} at 0.1 Hz.

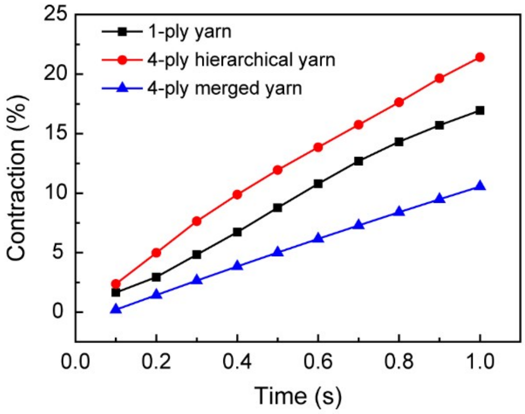

Figure S12. The contraction of single and multi-ply yarn muscles between 0-1.0 s.

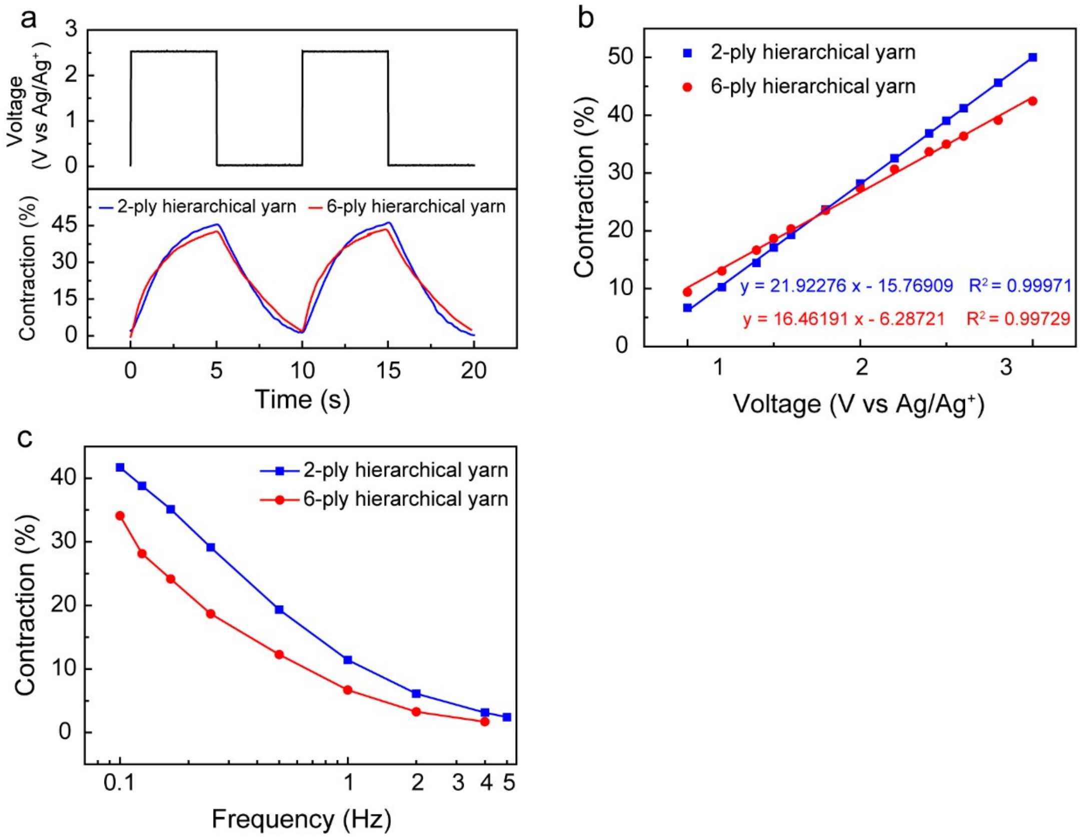

Figure S13. Characterization of electrochemical actuation of 2-ply hierarchical and 6-ply hierarchical yarn muscles. (a) Contraction response upon square-wave voltage signals. (b) The tensile contractions as a function of applied driving voltage for single and multiplied yarn muscles at 10 MPa and 0.1 Hz. (c) The dependence of tensile contractions on voltage on-off frequency for single and multi-ply yarn muscles. The voltage is 2.5 V and the applied stress is 10 MPa.

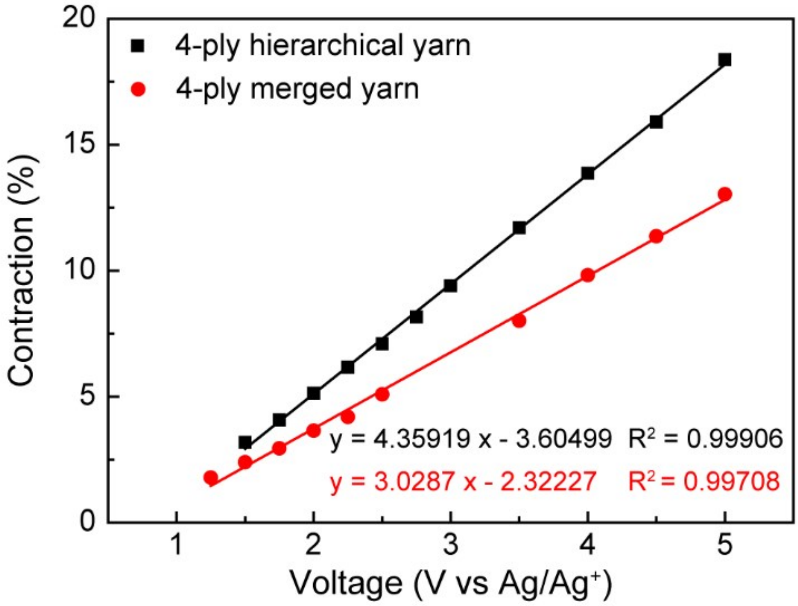

Figure S14. The tensile contractions as a function of applied driving voltage for 4-ply hierarchical yarn muscles and 4-ply merged yarn muscles at 1 Hz, under 10 MPa stress.

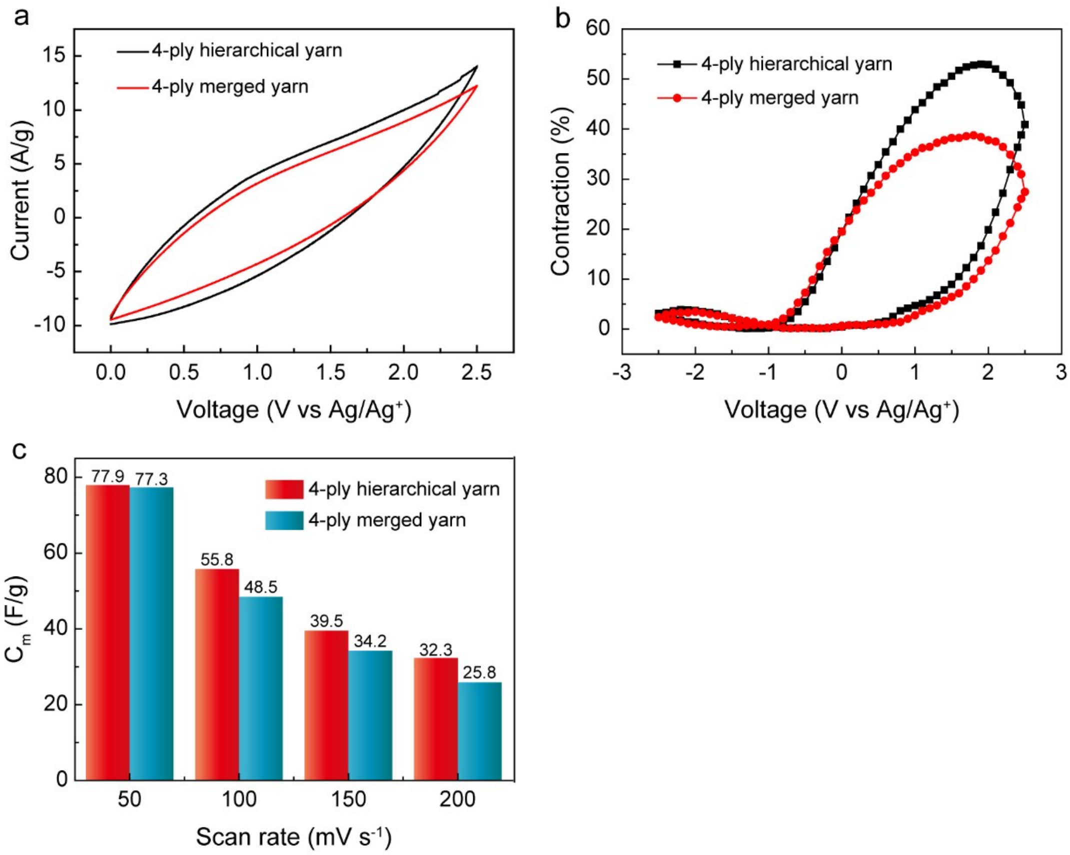

Figure S15. (a) Cyclic voltammetry curves of the 4-ply hierarchical CNT yarn and the 4-ply merged CNT yarn obtained at a scan rate of 200 mV/s. (b) The specific capacitance of the yarns obtained Drive response for cyclic voltammetry. (b) Tensile stroke of the yarn muscles during a cyclic voltammetry scan at 200 mV/s, under 10 MPa isobaric stress. (c) The capacitance vs scan rate during CV scans.

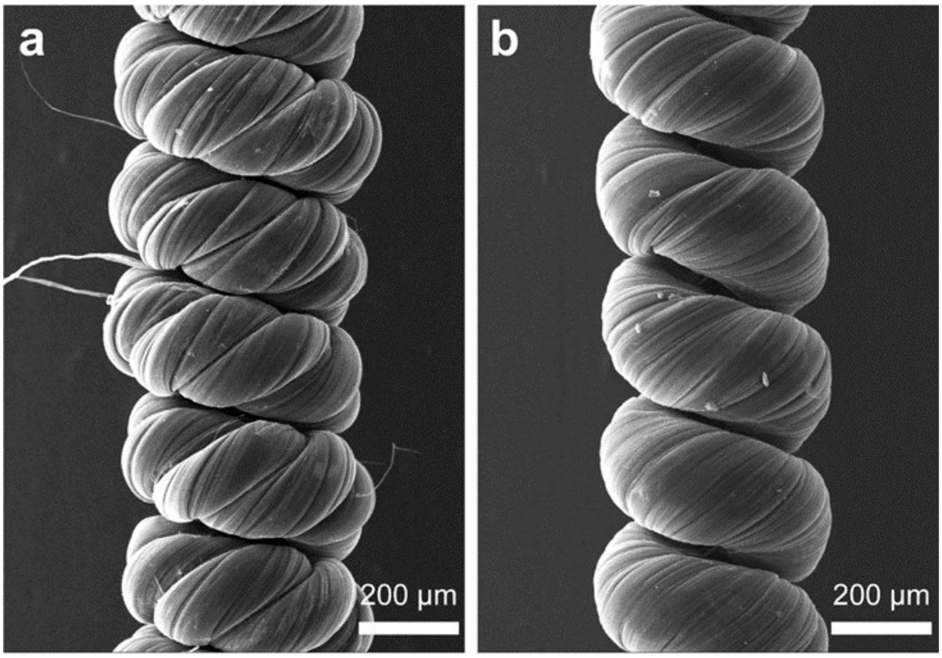

Figure S16. SEM images of (a) a thick 4-ply hierarchical yarn prepared using four twisted yarns that contain two CNT ribbons and (b) a 8-ply merged yarn prepared by stacking and twisting 8 CNT ribbons. The amount of CNTs in the two yarns is almost same.

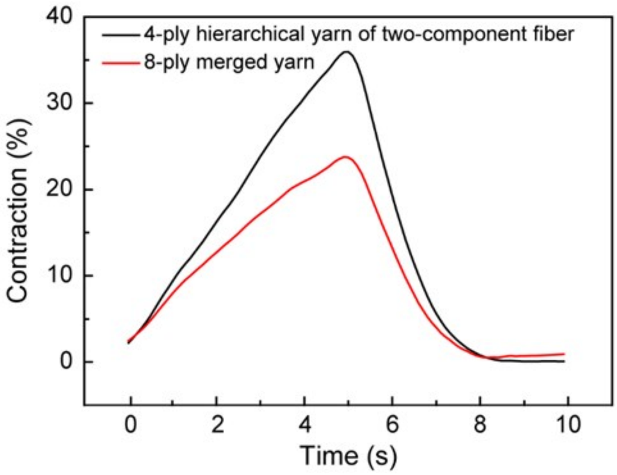

Figure S17. Contraction responses versus time for the thick 4-ply hierarchical yarn and the 8-ply merged yarn shown in Figure S16. The yarns were driven by a 0.1 Hz square wave voltage (0 to 2.5 V vs Ag/Ag^+) and the load was 9 MPa. The thick hierarchical yarn showed lower contraction than the 4-ply yarn in Fig. 3a, due to the increased thickness, its contraction was higher than that generated by the 8-ply merged yarn.

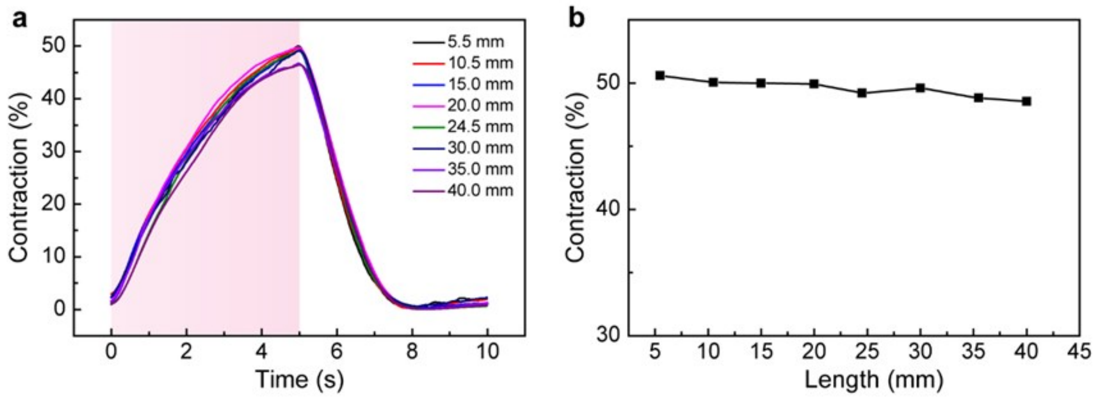

Figure S18. (a) Contraction versus time for the 4-ply hierarchical CNT yarns with the lengths from 5.5 to 40 mm. (b) The contraction versus muscle length obtained from (a). The yarns were driven by a 0.1 Hz square wave voltage (0 to 2.5 V vs Ag/Ag^{+}) and the load was 10 MPa. For the investigated length range, the actuation performance of the contraction and the contraction rate were almost independent on the muscle length. The length of 40 mm is the maximum that is allowed for actuation test in our setup for electrochemical actuation test. We rationally think that high lengthwise contraction displacement can be obtained by connecting the yarn muscles in series. The connecting points can be wired together using very soft wires to lower the negative effect induced by the increase of resistance when the muscle length is long.

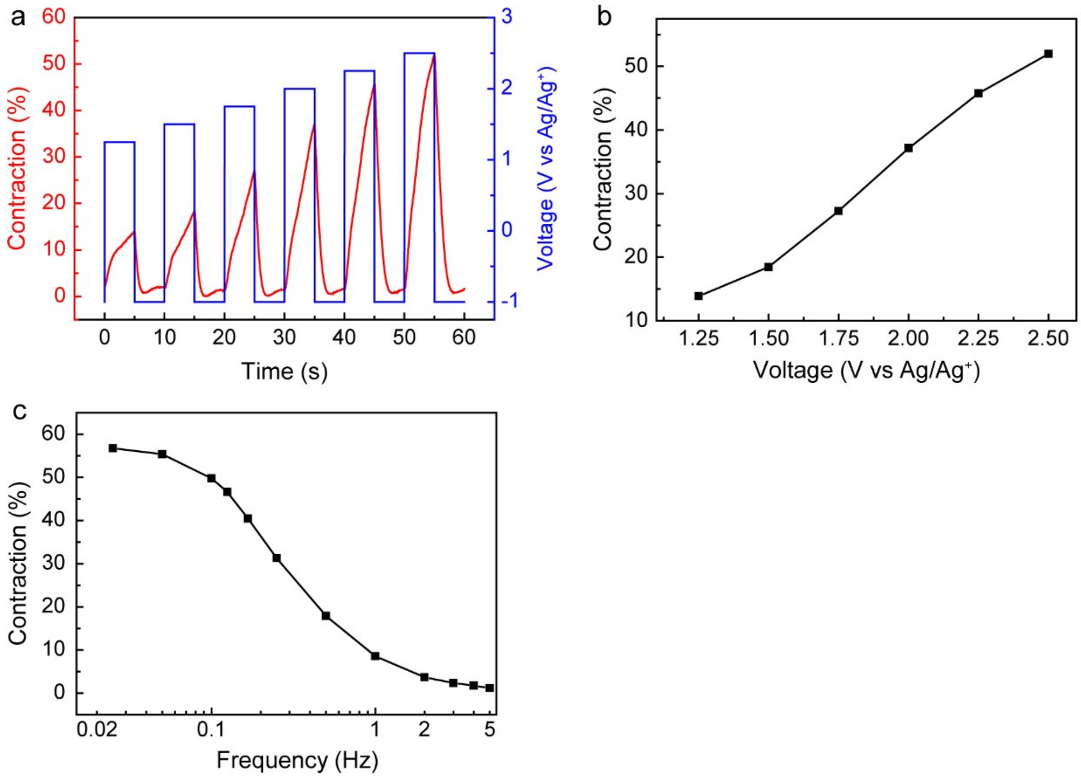

Figure S19. (a) The contraction(left) and applied voltage(right) vs time of 2-ply hierarchical yarn muscle with PAN membrane when the frequency is 0.1 Hz and the applied stress is 8.5 MPa. (b) The tensile contractions as a function of applied driving voltage for 2-ply hierarchical yarn muscle with PAN membrane at 0.1 Hz, under 8.5 MPa. (c)The dependence of tensile contractions on voltage on-off frequency for 2-ply hierarchical yarn muscle with PAN membrane. The voltage is 2.5 V and the applied stress is 8.5 MPa.

Table 1. Comparison of the tensile contraction and the contraction rate between the literature results for electrochemical yarn muscles and the present results for our 4-ply hierarchical yarn muscles

Materials	Electrolyte*	Applied voltage	Contraction	Rate [% s^{-1}]	Ref
CNT	$TEA\cdot BF_4$/PC	2.5V (two electrode)	1.3%	0.033	[1]
CNT	0.2 M $TBA\cdot PF_6$/PC	−3.25V (vs Ag/Ag^+)	16.5%	0.165	[2]
CNT/rGO	0.5 M Na_2SO_4 aqueous solution	−2V (vs SCE)	8.1%	2.7.	[3]
CNT/ graphene	0.2 M $TBA\cdot PF_6$/PC	−3V (vs Ag/Ag^+)	19%	0.127	[4]
CNT	0.2 M $THA\cdot PF_6$/PC	3.25V (vs Ag/Ag^+)	15.1%	2.32	[5]
Nylon/ CNT	0.2 M $TBA\cdot PF_6$/PC	−3V (two electrode)	14.3%	7.15	[6]
CNT	0.2 M $TEA\cdot BF_4$/PC	3V (vs Ag/Ag^+)	62.4%	23.8	This work

* $TEA\cdot BF_4$: Tetraethylammonium Tetrafluoroborate

$TBA\cdot BF_4$: Tetrabutylammonium Tetrafluoroborate

$TBA\cdot PF_6$: Tetrabutylammonium Hexafluorophosphate

$THA\cdot PF_6$: Tetrahexylammonium Hexafluorophosphate

PC: Propylene carbonate

References:

[1] J. A. Lee, Y. T. Kim, G. M. Spinks, D. Suh, X. Lepro, M. D. Lima, R. H. Baughman, S. J. Kim, Nano Lett 2014, 14, 2664.

[2] J. A. Lee, N. Li, C. S. Haines, K. J. Kim, X. Lepro, R. Ovalle-Robles, S. J. Kim, R. H. Baughman, Adv Mater 2017, 29, 7.

[3] J. Qiao, J. Di, S. Zhou, K. Jin, S. Zeng, N. Li, S. Fang, Y. Song, M. Li, R. H. Baughman, Q. Li, Small 2018, 14, e1801883.

[4] J. S. Hyeon, J. W. Park, R. H. Baughman, S. J. Kim, Sensors and Actuators B-Chemical 2019, 286, 237.

[5] K. J. Kim, J. S. Hyeon, H. Kim, T. J. Mun, C. S. Haines, N. Li, R. H. Baughman, S. J. Kim, ACS Appl Mater Interfaces 2019, 11, 13533.

[6] J. Mu, M. Jung de Andrade, S. Fang, X. Wang, E. Gao, N. Li, S. H. Kim, H. Wang, C. Hou, Q. Zhang, M. Zhu, D. Qian, H. Lu, D. Kongahage, S. Talebian, J. Foroughi, G. Spinks, H. Kim, T. H. Ware, H. J. Sim, D. Y. Lee, Y. Jang, S. J. Kim, R. H. Baughman, Science 2019, 365, 150.

Video S1 showing tensile actuation of the 4-ply hierarchical yarn muscle at a applied 0.1 Hz, 2.5 V square-wave voltage.

Video S2 showing four 4-ply hierarchical yarn muscles were connected in parallel contracted by 42.6% in length against a heavy load of 30 grams, when a voltage of 2.5 V, 0.1 Hz was applied.